Science Advances
AAAS

Supplementary Materials for

Enhanced ocean heat storage efficiency during the last deglaciation

Chenyu Zhu *et al.*

Corresponding author: Zhengyu Liu, liu.7022@osu.edu; Peter U. Clark, peter.clark@oregonstate.edu

Sci. Adv. **10**, eadp5156 (2024)
DOI: 10.1126/sciadv.adp5156

The PDF file includes:

Other Supplementary Material for this manuscript includes the following:

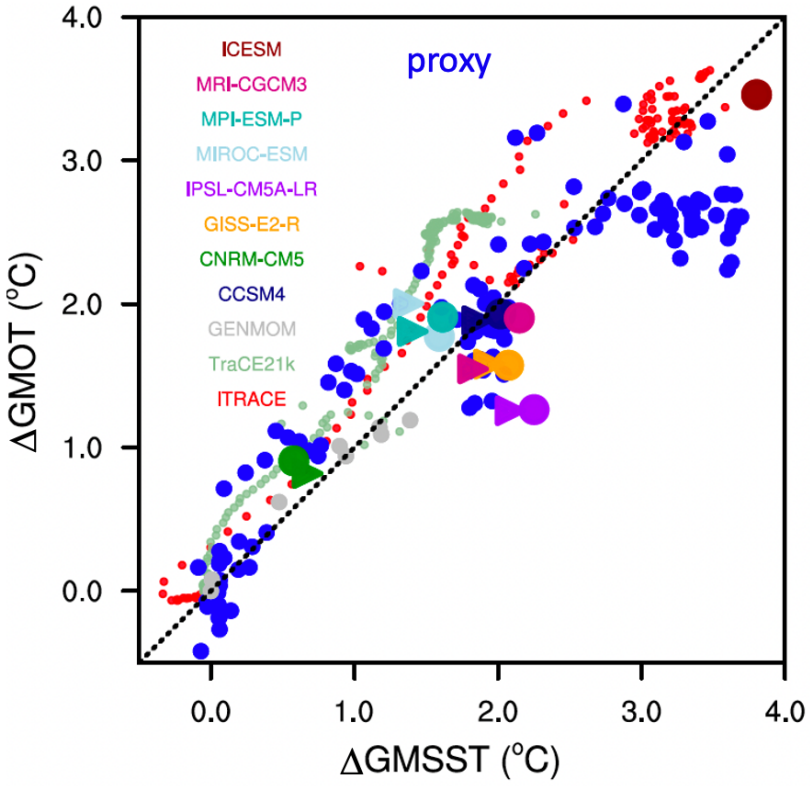

Figure S1. Scatter diagram between deglacial ΔGMSST and ΔGMOT. Reconstructions (blue dots)of ΔGMSST from 20ka to 6ka are from Shakun et al. (*19*) and Marcott et al. (*20*) and of ΔGMOT from Shackleton et al. (7). Also shown are results from two transient deglacial simulations iTRACE (20ka-6ka; red dots) and TraCE-21k (22ka-0ka; light green dots), eight time-slice simulations spanning the last deglaciation (*33*, gray) , and equilibrium simulations from seven PMIP3 models and iCESM (MH-LGM in filled triangles and PI-LGM in filled circles). The dashed black line denotes the HSE (ΔGMOT/ΔGMSST) =1.

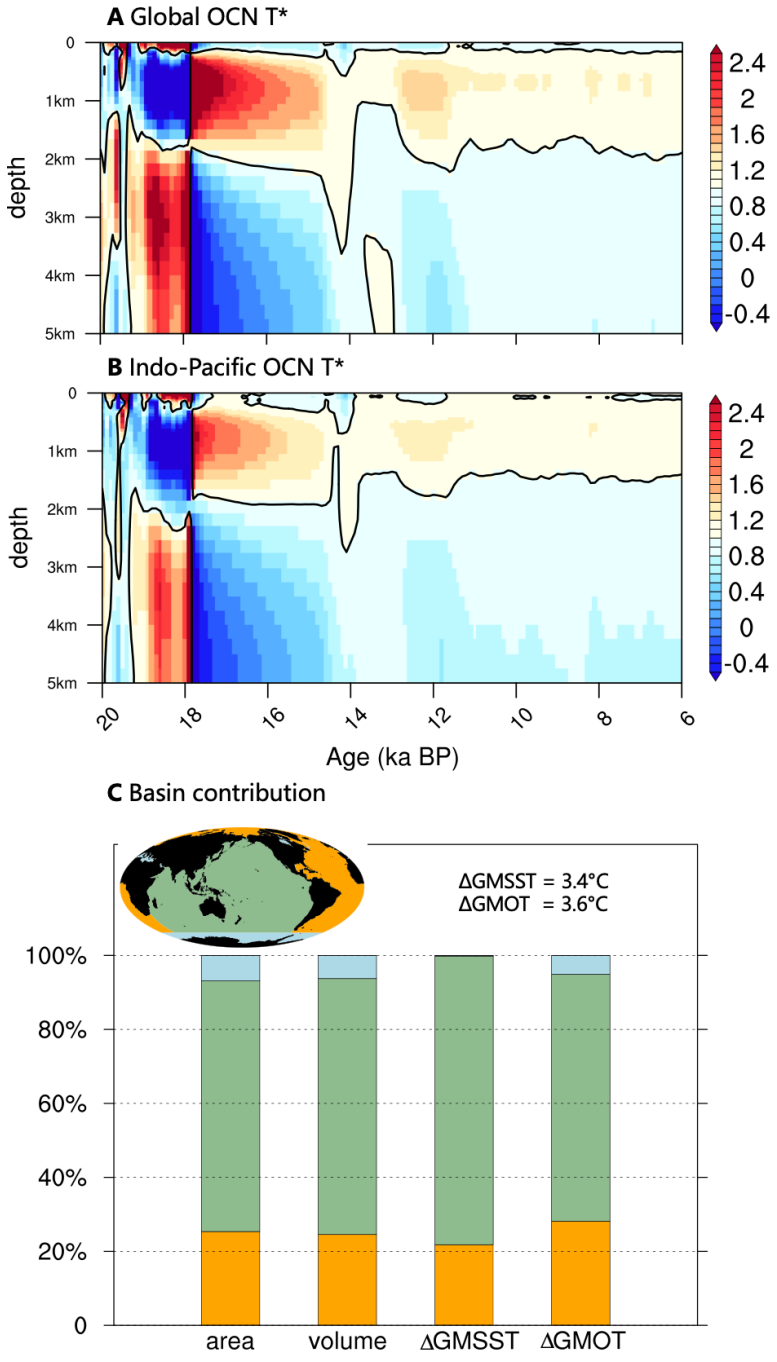

Figure S2. (**A**) Hovmöller diagram of scaled deglacial global mean ocean temperature changes (relative to the LGM, divided by transient ΔGMOT) as a function of time and depth. (**B**) as (A) but for the Indo-Pacific Ocean. Black contours in (A) and (B) highlight the value of 1. **(C)** Contributions (%) of individual basin to global ocean surface area, volume, ΔGMSST and ΔGMOT. Inserted graphic demonstrates the domain of each basin, with color corresponding to that of the bar chart.

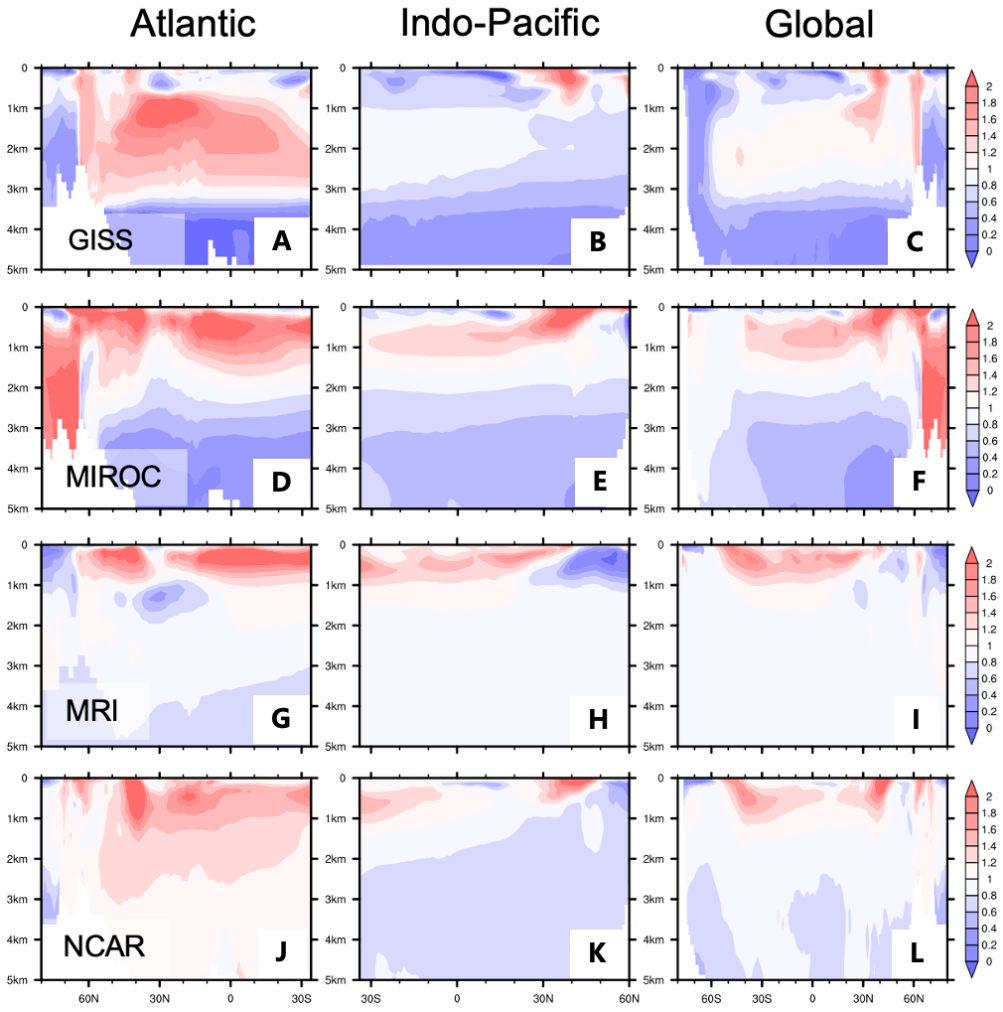

Figure S3. Scaled PI-LGM zonal mean ocean temperature change (divided by ΔGMSST) in the Atlantic (*left*), Indo-Pacific (*middle*) and global basin (*right*) in four representative PMIP3 models.

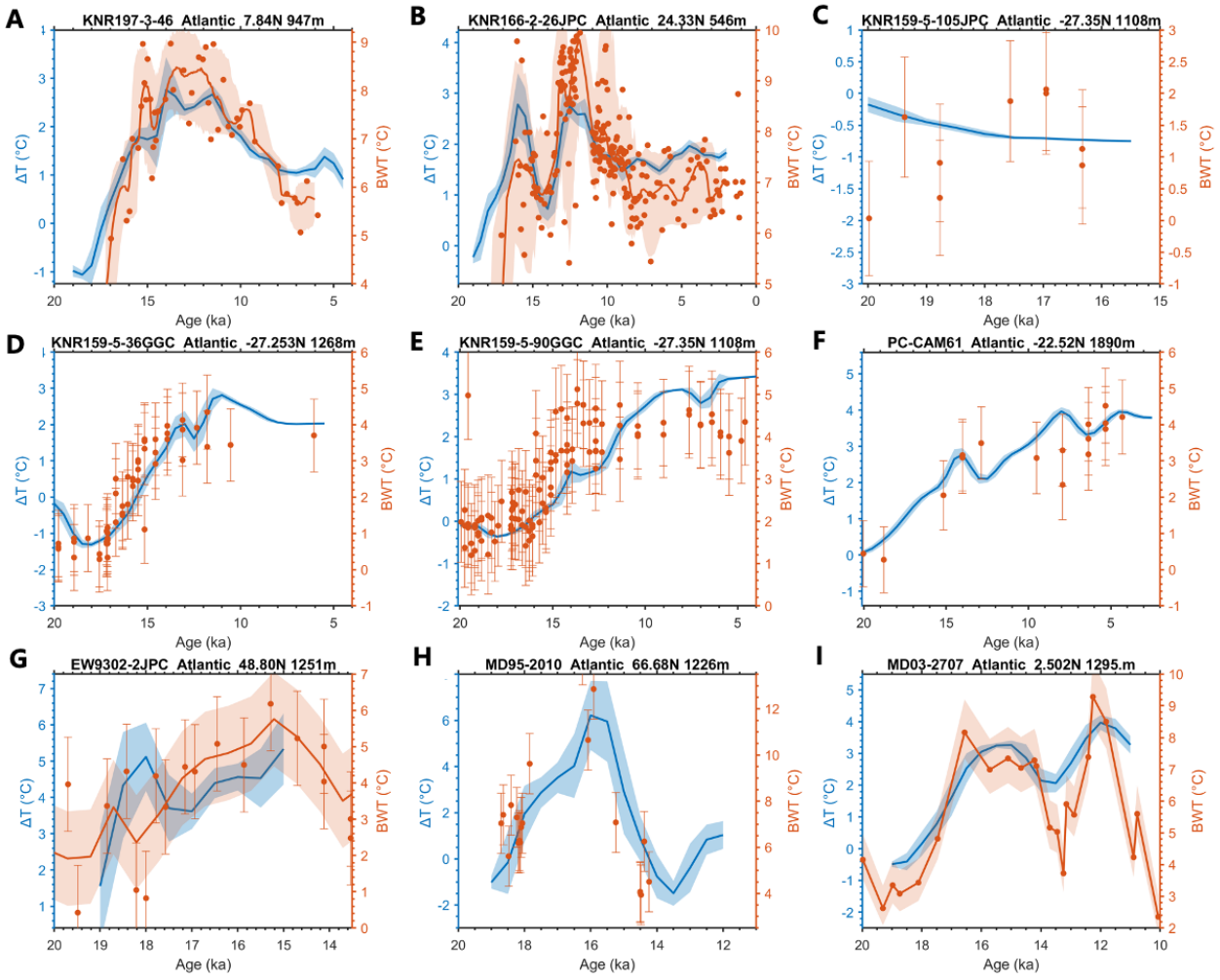

Figure S4. Temperature reconstructions from several Atlantic intermediate-depth sites (red) compared to our ΔDOT reconstructions (blue) for those sites. The reconstructions from (**A**) KNR197-3-46 (*63*), (**B**) KNR166-2-26JPC (*77*), (**C**) KNR-159-105JPC (*78*), (**D**) KNR159-5-36GGC (*78*), (**E**) KNR159-5-90GGC (*78*), and (**F**) PC-CAM61 (*78*) are based on the Mg/Li proxy. Temperature reconstructions for the other three cores are based on Mg/Ca: (**G**) EW9302-2JPC (*50*), (**H**) MD95-2010 (*50*), and (**I**) MD03-2707 (*51*).

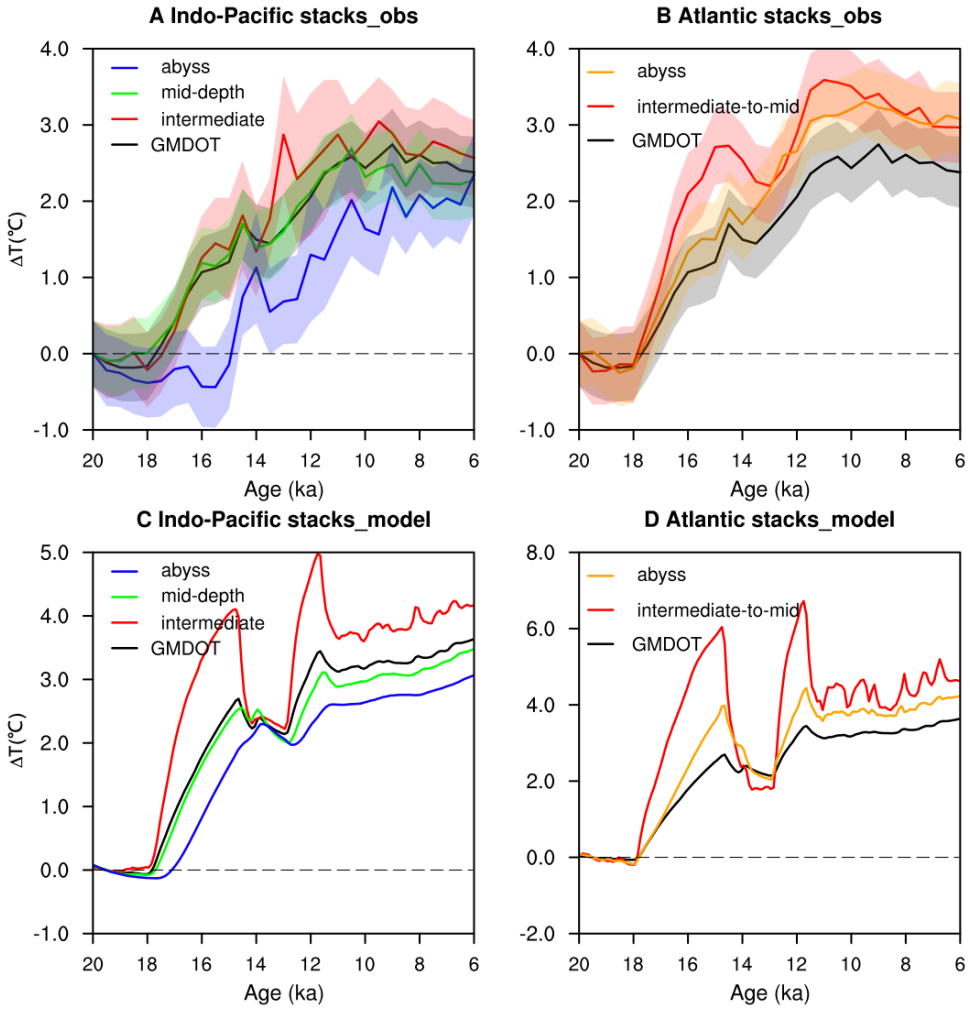

Figure S5. Model-data stacks comparison. See Fig. 2 for details on stack domain and color convention.

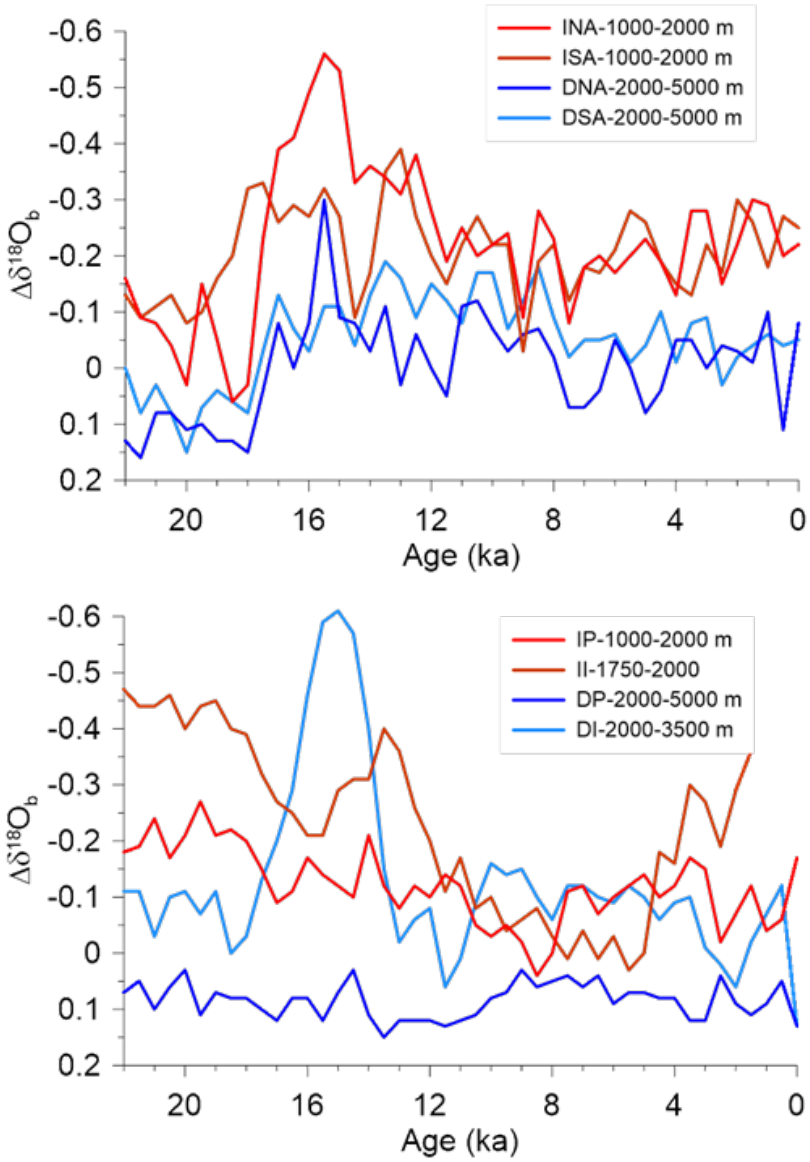

Figure S6. Differences between regional benthic $\delta^{18}O$ stacks and the global $\delta^{18}O$ stack. Upper panel is for the Atlantic and lower panel is for the Pacific and Indian Ocean. Acronyms are intermediate = I, deep = D, NA = North Atlantic, SA = South Atlantic, P =Pacific and I = Indian Ocean. Data from Lisiecki and Stern (*36*).

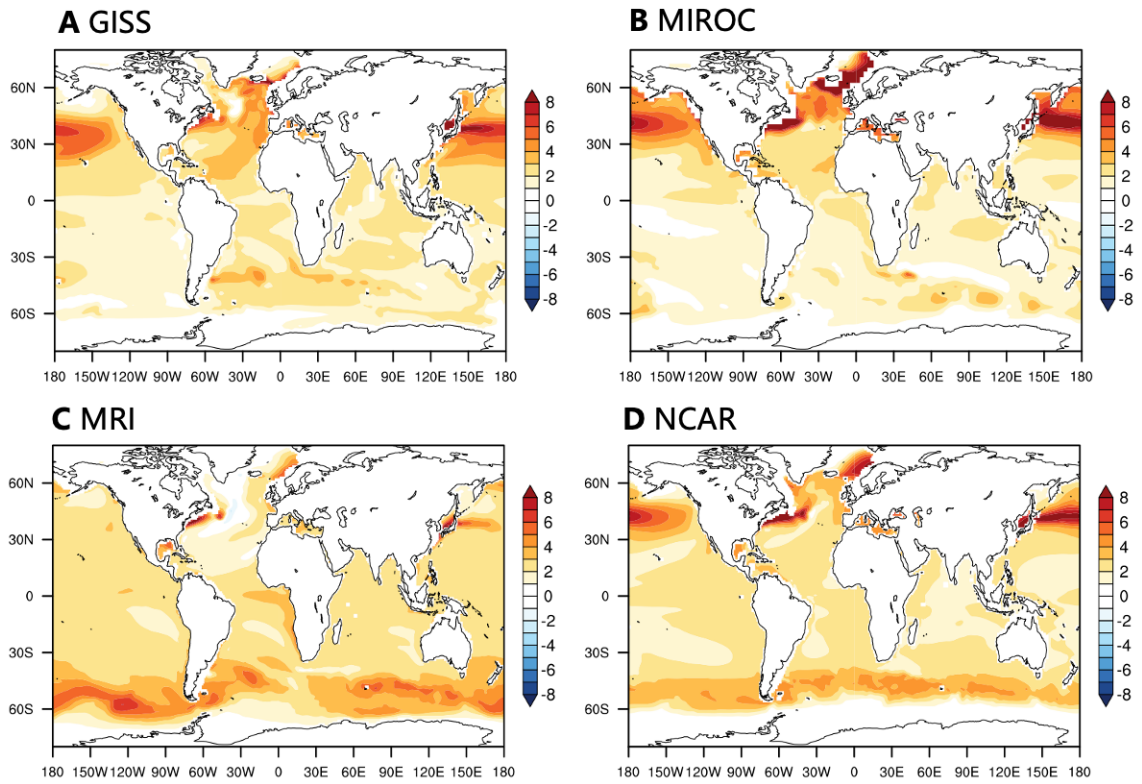

Figure S7. PI-LGM SST change (units: °C) in four representative PMIP3 models.

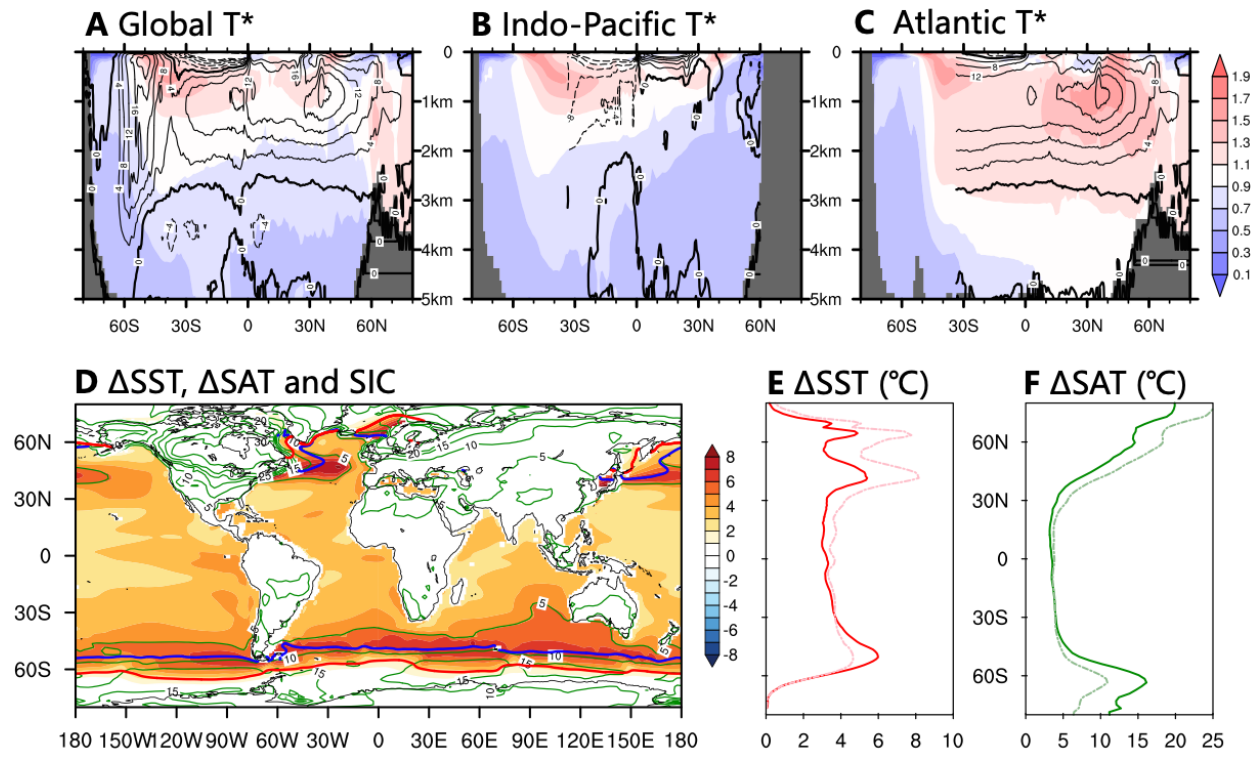

Figure S8. ICE+ORB+GHG simulated deglacial temperature changes. (**A-C**) Scaled zonal mean ocean temperature change between the MH and LGM (divided by ΔGMSST) in the global ocean (A), Indo-Pacific (B) and Atlantic (C). Contours in (A-C) show overturning stream-function in the MH in each basin (interval of 4 Sv). (**D**) Changes in annual mean surface air temperature (SAT, green contour, interval of 5°C) and annual mean SST (color shading, °C). Blue and red lines indicate sea ice edge (defined as 15% annual sea ice coverage) in the LGM (blue) and the MH (red). (**E**) Zonal mean change of annual SST in iTRACE (solid line) and a reanalysis product (dashed line) (*31*). (**F**) As (E) but for SAT.

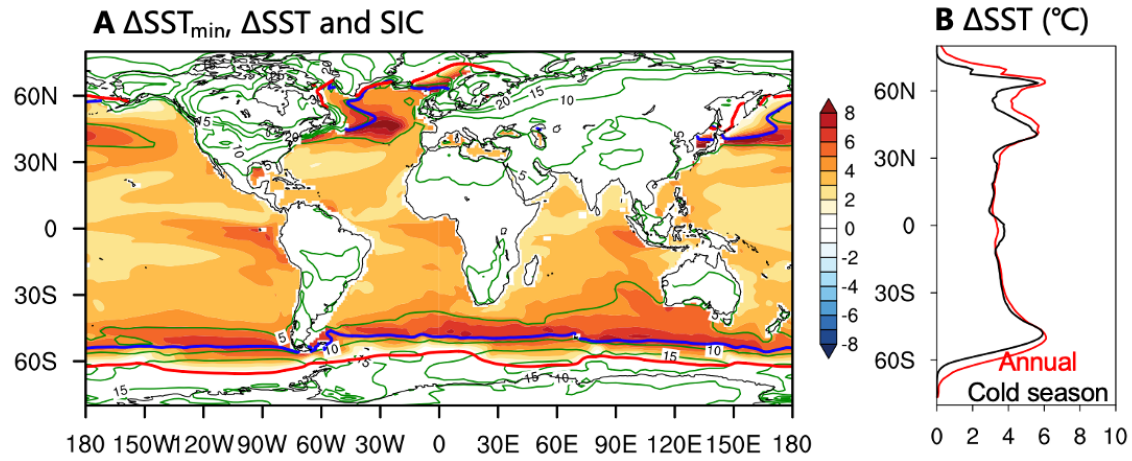

Figure S9. (**A**) MH-LGM changes in annual mean surface air temperature (SAT, green contour, interval of 5°C) and *cold season* SST (shading, °C) simulated in iTRACE. Blue and red lines indicate sea ice edge (defined as 15% annual sea ice coverage) at the LGM (blue) and MH (red), respectively. (**B**) Zonal mean change (MH-LGM) of cold season SST (black) and annual mean SST (red).

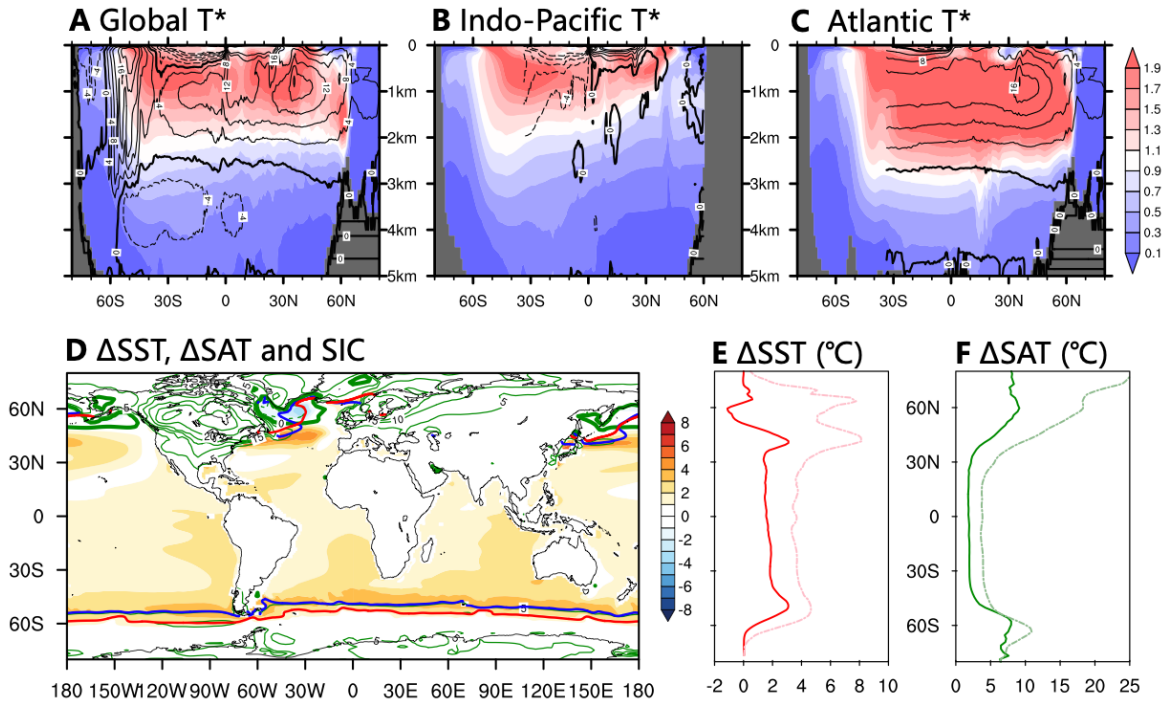

Figure S10. As Figure S8 but for ICE run.

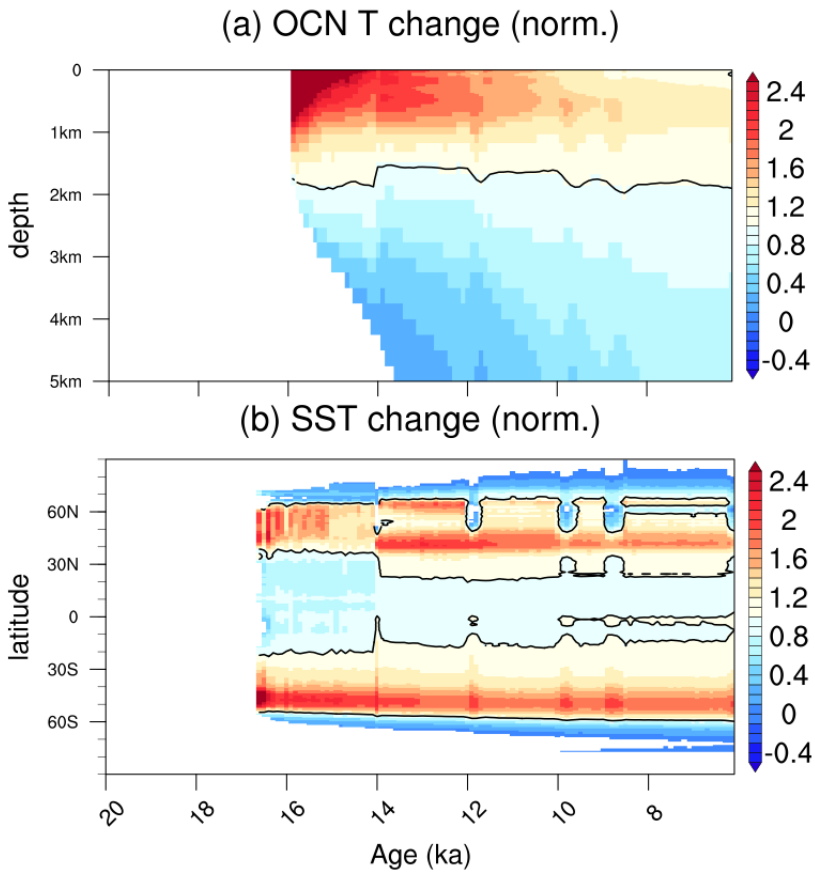

Figure S11 (a) Hovmöller diagram of deglacial global mean ocean temperature changes (relative to the LGM, normalized by ΔGMOT) in ICE+ORB+GHG run as a function of time and depth. (b) As (a) but for zonal mean SST changes (relative to the LGM, normalized by ΔGMSST) as a function of time and latitude. Only temperature changes larger than 0.1 °C (relative to the LGM state) are considered.

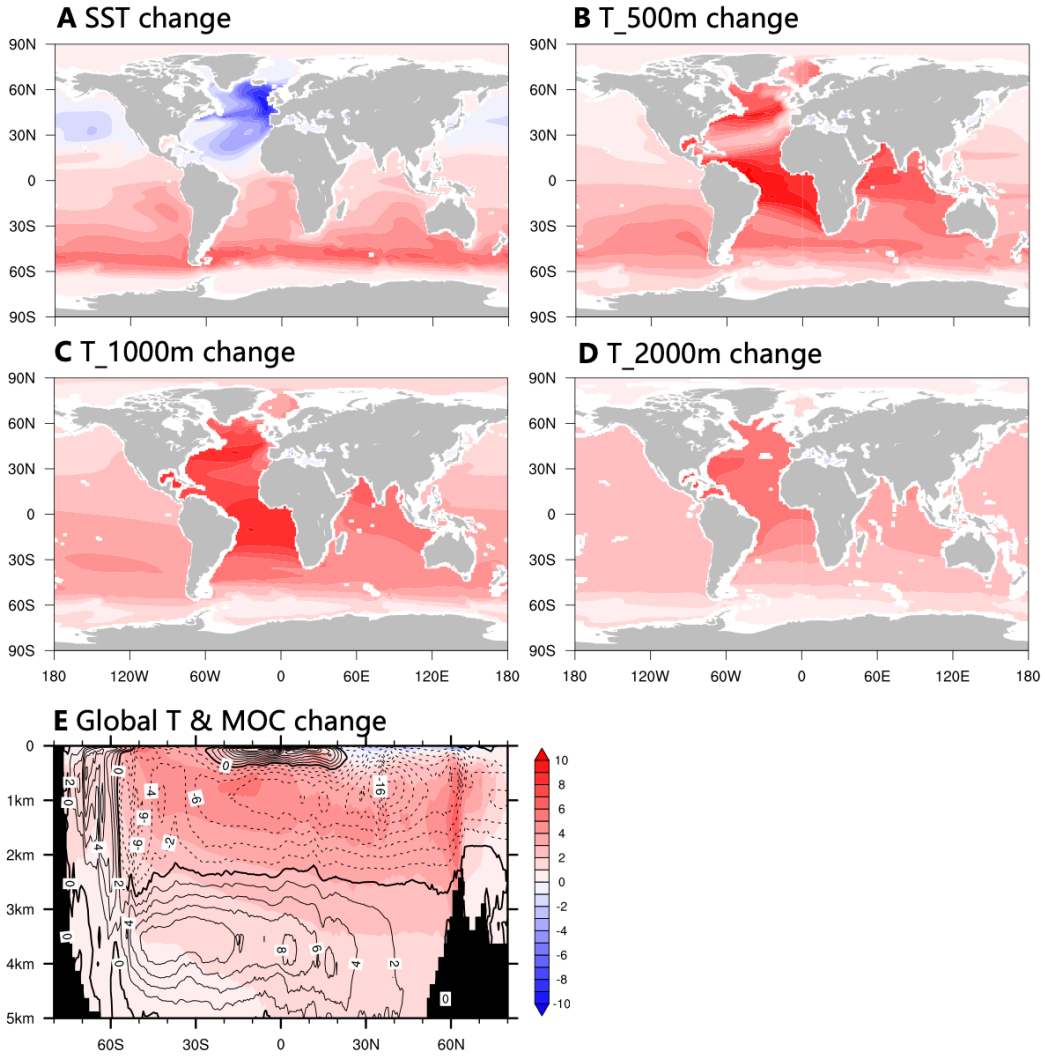

Figure S12. (**A**) SST changes (°C) between 15-14.9ka and 19ka in iTRACE. (**B**) As (A) but for temperature changes (°C) at 500-m depth. (**C**) As (A) but for temperature change at 1000-m depth. (**D**) As (A) but for temperature change at 2000-m depth. (**E**) Zonal mean Atlantic temperature (shading; °C) and overturning circulation (contour; interval of 2 Sv) changes between 15-14.9ka and 19ka in iTRACE.

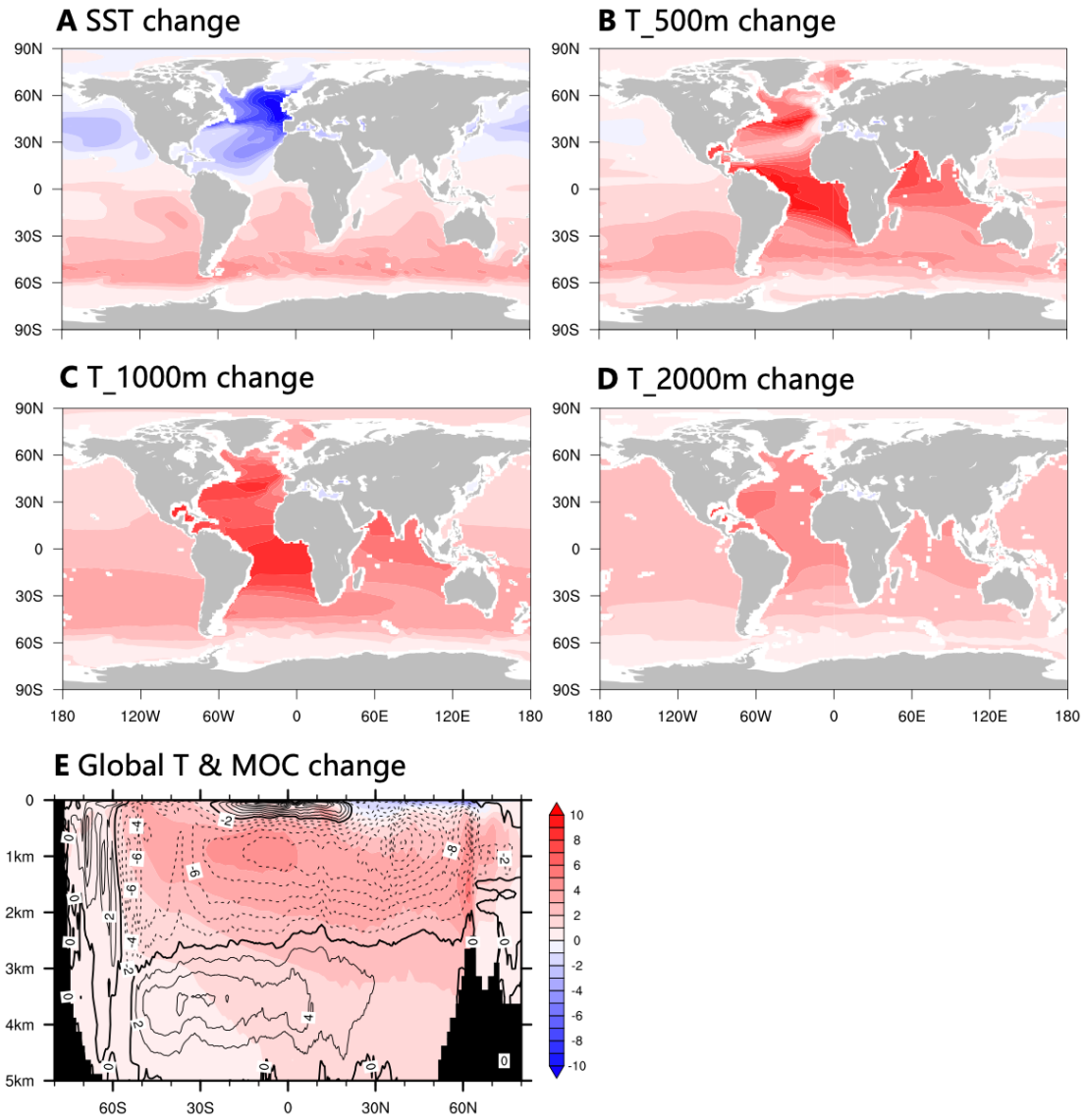

Figure S13. As Figure S12 but highlighting the pure meltwater effect by iTRACE minus ICE+ORB+GHG run. Note the patterns are very similar to Figure S12.

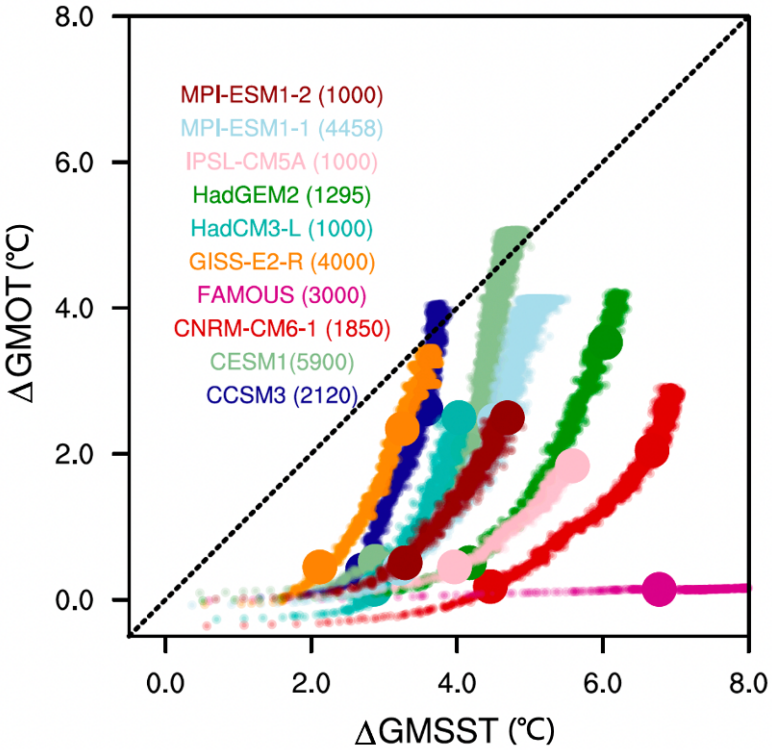

Figure S14. Scatter diagram between GMSST change and GMOT change (units: °C) in LongRunMIP abrupt4x experiments. Length of each simulation is shown in bracket. Large dots highlight year 100 and year 1000 for each simulation.

Table S1. Simulated PI-LGM GMSST and GMOT changes in PMIP3 and iCESM1 models

Model	ΔGMSST (°C)	ΔGMOT (°C)	ΔGMOT /ΔGMSST
CCSM4	2.0	1.9	1.0
CNRM-CM5	0.6	0.9	1.5
GISS-E2-R	2.1	1.6	0.8
IPSL-CM5A-LR	2.3	1.3	0.6
MIROC-ESM	1.6	1.8	1.1
MPI-ESM-P	1.6	1.9	1.2
MRI-CGCM3	2.1	1.9	0.9
iCESM1	3.8	3.5	0.9

Data S1. Tab 1 ("Metadata"): the metadata for the 119 benthic $\delta^{18}O$ records used to calculate ΔDOT and ΔGMDOT. Tab 2 ("Global and Regional Stacks"): the global and regional ΔDOT stacks and their uncertainties. Tab 3 (labeled "$d^{18}O$ 500 years"): the $\delta^{18}O$ stack (0 - 20 ka) at 500-year resolution.

REFERENCES AND NOTES

1. J. M. Gregory, R. J. Stouffer, S. C. B. Raper, P. A. Stott, N. A. Rayner, An observationally based estimate of the climate sensitivity. *J. Climate* **15**, 3117–3121 (2002).

2. J. Hansen, L. Nazarenko, R. Ruedy, M. Sato, J. Willis, A. Del Genio, D. Koch, A. Lacis, K. Lo, S. Menon, T. Novakov, J. Perlwitz, G. Russell, G. A. Schmidt, N. Tausnev, Earth's energy imbalance: Confirmation and implications. *Science* **308**, 1431–1435 (2005).

3. S. Levitus, J. I. Antonov, T. P. Boyer, O. K. Baranova, H. E. Garcia, R. A. Locarnini, A. V. Mishonov, J. R. Reagan, D. Seidov, E. S. Yarosh, M. M. Zweng, World ocean heat content and thermosteric sea level change (0–2000 m), 1955–2010. *Geophys. Res. Lett.* **39**, doi.org/10.1029/2012GL051106 (2012).

4. M. Rhein, S. R. Rintoul, S. Aoki, E. Campos,D. Chambers, R. A. Feely, S. Gulev, G. C. Johnson, S. A. Josey, A. Kostianoy, C. Mauritzen, D. Roemmich, L. D. Talley, F. Wang, "Observations: Ocean" in *Climate Change 2013: The Physical Science Basis. Contribution of Working Group I to the Fifth Assessment Report of the Intergovernmental Panel on Climate Change*, T. F. Stocker, D. Qin, G.-K. Plattner, M. Tignor, S. K. Allen, J. Boschung, A. Nauels, Y. Xia, V. Bex, P. M. Midgley, Eds. (Cambridge Univ. Press, 2013), pp. 255–315.

5. L. Cheng, J. Abraham, K. E. Trenberth, T. Boyer, M. E. Mann, J. Zhu, F. Wang, F. Yu, R. Locarnini, J. Fasullo, F. Zheng, Y. Li, B. Zhang, L. Wan, X. Chen, D. Wang, L. Feng, X. Song, Y. Liu, F. Reseghetti, S. Simoncelli, V. Gouretski, G. Chen, A. Mishonov, J. Reagan, K. von Schuckmann, Y. Pan, Z. Tan, Y. Zhu, W. Wei, G. Li, Q. Ren, L. Cao, Y. Lu, New record ocean temperatures and related climate indicators in 2023. *Adv. Atmos. Sci.* **41**, 1068–1082 (2024).

6. E. D. Galbraith, T. M. Merlis, J. B. Palter, Destabilization of glacial climate by the radiative impact of Atlantic meridional overturning circulation disruptions. *Geophys. Res. Lett.* **43**, 8214–8221 (2016).

7. S. Shackleton, A. Seltzer, D. Baggenstos, L. Lisiecki, Benthic $\delta^{18}O$ records Earth's energy imbalance. *Nat. Geosci.* **16**, 797–802 (2023).

8. K. von Schuckmann, A. Minière, F. Gues, F. J. Cuesta-Valero, G. Kirchengast, S. Adusumilli, F. Straneo, M. Ablain, R. P. Allan, P. M. Barker, H. Beltrami, A. Blazquez, T. Boyer, L. Cheng, J. Church, D. Desbruyeres, H. Dolman, C. M. Domingues, A. García-García, D. Giglio, J. E. Gilson, M. Gorfer, L. Haimberger, M. Z. Hakuba, S. Hendricks, S. Hosoda, G. C. Johnson, R. Killick, B. King, N. Kolodziejczyk, A. Korosov, G. Krinner, M. Kuusela, F. W. Landerer, M. Langer, T. Lavergne, I. Lawrence, Y. Li, J. Lyman, F. Marti, B. Marzeion, M. Mayer, A. H. MacDougall, T. McDougall, D. P. Monselesan, J. Nitzbon, I. Otosaka, J. Peng, S. Purkey, D. Roemmich, K. Sato, K. Sato, A. Savita, A. Schweiger, A. Shepherd, S. I. Seneviratne, L. Simons, D. A. Slater, T. Slater, A. K. Steiner, T. Suga, T. Szekely, W. Thiery, M.-L. Timmermans, I. Vanderkelen, S. E. Wjiffels, T. Wu, M. Zemp, Heat stored in the Earth system 1960–2020: Where does the energy go? *Earth Syst. Sci. Data* **15**, 1675–1709 (2023).

9. S. K. Gulev, P. W. Thorne, J. Ahn, F. J. Dentener, C. M. Domingues, S. Gerland, D. Gong, D. S. Kaufman, H. C. Nnamchi, J. Quaas, J. A. Rivera, S. Sathyendranath, S. L. Smith, B. Trewin, K. von Schuckmann, R. S. Vose, "Changing state of the climate system" in *Climate Change 2021: The Physical Science Basis. Contribution of Working Group I to the Sixth Assessment Report of the Intergovernmental Panel on Climate Change*, V. Masson-Delmotte, P. Zhai, A. Pirani, S. L. Connors, C. Péan, S. Berger, N. Caud, Y. Chen, L. Goldfarb, M. I. Gomis, M. Huang, K. Leitzell, E. Lonnoy, J. B. R. Matthews, T. K. Maycock, T. Waterfield, O. Yelekçi, R. Yu, B. Zhou, Eds. (Cambridge Univ. Press, 2021), pp. 287−422.

10. M. Rugenstein, J. Bloch-Johnson, A. Abe-Ouchi, T. Andrews, U. Beyerle, L. Cao, T. Chadha, G. Danabasoglu, J.-L. Dufresne, L. Duan, M.-A. Foujols, T. Frölicher, O. Geoffroy, J. Gregory, R. Knutti, C. Li, A. Marzocchi, T. Mauritsen, M. Menary, E. Moyer, L. Nazarenko, D. Paynter, D. Saint-Martin, G. A. Schmidt, A. Yamamoto, S. Yang, LongRunMIP—Motivation and design for a large collection of millennial-length GCM simulations. *Bull. Am. Meteorol. Soc.* **100**, 2551–2570 (2019).

11. Y. Rosenthal, B. K. Linsley, D. W. Oppo, Pacific Ocean heat content during the past 10,000 years. *Science* **342**, 617–620 (2013).

12. G. Gebbie, P. Huybers, The Little Ice Age and 20th-century deep Pacific cooling. *Science* **363**, 70–74 (2019).

13. A. Bagnell, T. DeVries, 20th century cooling of the deep ocean contributed to delayed acceleration of Earth's energy imbalance. *Nat. Commun.* **12**, 4604 (2021).

14. H. Elderfield, P. Ferretti, M. Greaves, S. Crowhurst, I. N. McCave, D. Hodell, A. M. Piotrowski, Evolution of ocean temperature and ice volume through the mid-Pleistocene climate transition. *Science* **337**, 704–709 (2012).

15. J. D. Shakun, D. W. Lea, L. E. Lisiecki, M. E. Raymo, An 800-kyr record of global surface ocean $\delta^{18}O$ and implications for ice volume-temperature coupling. *Earth Planet. Sci. Lett.* **426**, 58–68 (2015).

16. E. J. Rohling, G. L. Foster, T. M. Gernon, K. M. Grant, D. Heslop, F. D. Hibbert, A. P. Roberts, J. Yu, Comparison and synthesis of sea-level and deep-seatemperature variations over the past 40 million years. *Rev. Geophys.* **60**, e2022RG000775 (2022).

17. B. Bereiter, S. Shackleton, D. Baggenstos, K. Kawamura, J. Severinghaus, Mean global ocean temperatures during the last glacial transition. *Nature* **553**, 39–44 (2018).

18. M. Häberli, D. Baggenstos, J. Schmitt, M. Grimmer, A. Michel, T. Kellerhals, H. Fischer, Snapshots of mean ocean temperature over the last 700,000 years using noble gases in the EPICA Dome C ice core. *Clim. Past* **17**, 843–867 (2021).

19. J. D. Shakun, P. U. Clark, F. He, S. A. Marcott, A. C. Mix, Z. Liu, B. Otto-Bliesner, A. Schmittner, E. Bard, Global warming preceded by increasing carbon dioxide concentrations during the last deglaciation. *Nature* **484**, 49–54 (2012).

20. S. A. Marcott, J. D. Shakun, P. U. Clark, A. C. Mix, A reconstruction of regional and global temperature for the past 11,300 years. *Science* **339**, 1198–1201 (2013).

21. J. E. Tierney, J. Zhu, J. King, S. B. Malevich, G. J. Hakim, C. J. Poulsen, Glacial cooling and climate sensitivity revisited. *Nature* **584**, 569–573 (2020).

22. P. U. Clark, J. D. Shakun, Y. Rosenthal, P. Köhler, P. J. Bartlein, Global and regional temperature change over the past 4.5 million years. *Science* **383**, 884–890 (2024).

23. A. M. Seltzer, P. W. Davidson, S. A. Shackleton, D. P. Nicholson, S. Khatiwala, Global ocean cooling of 2.3°C during the Last Glacial Maximum. *Geophys. Res. Lett.* **51**, e2024GL108866 (2024).

24. C. Emiliani, Temperatures of Pacific bottom waters and polar superficial waters during the Tertiary. *Science* **119**, 853–855 (1954).

25. J. Hansen, M. Sato, G. Russell, P. Kharecha, Climate sensitivity, sea level and atmospheric carbon dioxide. *Phil. Trans. R. Soc. A.* **371**, 20120294 (2013).

26. J. E. Hansen, M. Sato, L. Simons, L. S. Nazarenko, I. Sangha, P. Kharecha, J. C. Zachos, K. von Schuckmann, N. G. Loeb, M. B. Osman, Q. Jin, G. Tselioudis, E. Jeong, A. Lacis, R. Ruedy, G. Russell, J. Cao, J. Li, Global warming in the pipeline. *Oxford Open Clim. Change* **3**, kgad008 (2023).

27. N. Maffezzoli, P. Vallelonga, R. Edwards, A. Saiz-Lopez, C. Turetta, H. A. Kjær, C. Barbante, B. Vinther, A. Spolaor, A 120 000-year record of sea ice in the North Atlantic? *Clim. Past* **15**, 2031–2051 (2019).

28. X. Crosta, K. E. Kohfeld, H. C. Bostock, M. Chadwick, A. Du Vivier, O. Esper, J. Etourneau, J. Jones, A. Leventer, J. Müller, R. H. Rhodes, C. S. Allen, P. Ghadi, N. Lamping, C. B. Lange, K.-A. Lawler, D. Lund, A. Marzocchi, K. J. Meissner, L. Menviel, A. Nair, M. Patterson, J. Pike, J. G. Prebble, C. Riesselman, H. Sadatzki, L. C. Sime, S. K. Shukla, L. Thöle, M.-E. Vorrath, W. Xiao, J. Yang, Antarctic sea ice over the past 130 000 years—Part 1: A review of what proxy records tell us. *Clim. Past* **18**, 1729–1756 (2022).

29. E. C. Brady, S. Stevenson, D. Bailey, Z. Liu, D. Noone, J. Nusbaumer, B. L. Otto-Bliesner, C. Tabor, R. Tomas, T. Wong, J. Zhang, J. Zhu, The connected isotopic water cycle in the Community Earth System Model version 1. *J. Adv. Model. Earth Syst.* **11**, 2547–2566 (2019).

30. C. He, Z. Liu, B. L. Otto-Bliesner, E. C. Brady, C. Zhu, R. Tomas, P. U. Clark, J. Zhu, A. Jahn, S. Gu, J. Zhang, J. Nusbaumer, D. Noone, H. Cheng, Y. Wang, M. Yan, Y. Bao, Hydroclimate footprint of pan-Asian monsoon water isotope during the last deglaciation. *Sci. Adv.* **7**, eabe2611 (2021).

31. M. B. Osman, J. E. Tierney, J. Zhu, R. Tardif, G. J. Hakim, J. King, C. J. Poulsen, Globally resolved surface temperatures since the Last Glacial Maximum. *Nature* **599**, 239–244 (2021).

32. Z. Liu, B. L. Otto-Bliesner, F. He, E. C. Brady, R. Tomas, P. U. Clark, A. E. Carlson, J. Lynch-Stieglitz, W. Curry, E. Brook, D. Erickson, R. Jacob, J. Kutzbach, J. Cheng, Transient simulation of last deglaciation with a new mechanism for Bølling-Allerød warming. *Science* **325**, 310–314 (2009).

33. J. R. Alder, S. W. Hostetler, Global climate simulations at 3000-year intervals for the last 21 000 years with the GENMOM coupled atmosphere–ocean model. *Clim. Past* **11**, 449–471 (2015).

34. P. Braconnot, S. P. Harrison, M. Kageyama, P. J. Bartlein, V. Masson-Delmotte, A. Abe-Ouchi, B. Otto-Bliesner, Y. Zhao, Evaluation of climate models using palaeoclimatic data. *Nat. Clim. Chang.* **2**, 417–424 (2012).

35. J. Muglia, S. Mulitza, J. Repschläger, A. Schmittner, L. Lembke-Jene, L, Lisiecki, A. Mix, R. Saraswat, E. Sikes, C. Waelbroeck, J. Gottschalk, J. Lippold, D. Lund, G. Martinez-Mendez, E. Michel, F. Muschitiello, S. Naik, Y. Okazaki, L. Stott, A. Voelker, N. Zhao, A global synthesis of high-resolution stable isotope data from benthic foraminifera of the last deglaciation. *Sci. Data.* **10**, 131 (2023).

36. L. E. Lisiecki, J. V. Stern, Regional and global benthic $\delta^{18}O$ stacks for the last glacial cycle. *Paleoceanography* **31**, 1368–1394 (2016).

37. CLI MAP Project Members, The surface of the ice-age Earth: Quantitative geologic evidence is used to reconstruct boundary conditions for the climate 18,000 years ago. *Science* **191**, 1131–1137 (1976).

38. M. Kucera, M. Weinelt, T. Kiefer, U. Pflaumann, A. Hayes, M. Weinelt, M. Chen, A. C. Mix, T. T. Barrows, E. Cortijo, J. Duprat, S. Juggins, C. Waelbroeck, Reconstruction of the glacial Atlantic and Pacific sea-surface temperatures from assemblages of planktonic foraminifera: Multi-technique approach based on geographically constrained calibration datasets. *Quat. Sci. Rev.* **24**, 951–998 (2005).

39. MARGO Project Members, Constraints on the magnitude and patterns of ocean cooling at the Last Glacial Maximum. *Nat. Geosci.* **2**, 127–132 (2009).

40. J. D. Annan, J. C. Hargreaves, A new global reconstruction of temperature changes at the Last Glacial Maximum. *Clim. Past* **9**, 367–376 (2013).

41. J. D. Annan, J. C. Hargreaves, T. Mauritsen, A new global surface temperature reconstruction for the Last Glacial Maximum. *Clim. Past* **18**, 1883–1896 (2022).

42. L. Back, K. Russ, Z. Liu, K. Inoue, J. Zhang, B. L. Otto-Bliesner, Global hydrological cycle response to rapid and slow global warming. *J. Climate* **22**, 8781–8786 (2013).

43. E. Newsom, L. Zanna, S. Khatiwala, J. M. Gregory, The influence of warming patterns on passive ocean heat uptake. *Geophys. Res. Lett.* **47**, e2020GL088429 (2020).

44. L. Zanna, S. Khatiwala, J. M. Gregory, J. Ison, P. Heimbach, Global reconstruction of historical ocean heat storage and transport. *Proc. Natl. Acad. Sci. U.S.A.* **116**, 1126–1131 (2019).

45. J. F. McManus, R. Francois, J. Gherardi, L. D. Keigwin, S. Brown-Leger, Collapse and rapid resumption of Atlantic meridional circulation linked to deglacial climate changes. *Nature* **428**, 834–837 (2004).

46. J. Lippold, F. Pöppelmeier, F. Süfke, M. Gutjahr, T. J. Goepfert, P. Blaser, O. Friedrich, J. M. Link, L. Wacker, S. Rheinberger, S. L. Jaccard, Constraining the variability of the Atlantic meridional overturning circulation during the Holocene. *Geophys. Res. Lett.* **46**, 11338–11346 (2019).

47. W. S. Broecker, Paleocean circulation during the last deglaciation: A bipolar seesaw? *Paleoceanography* **13**, 119–121 (1998).

48. P. U. Clark, N. G. Pisias, T. F. Stocker, A. J. Weaver, The role of the thermohaline circulation in abrupt climate change. *Nature* **415**, 863–869 (2002).

49. T. F. Stocker, S. J. Johnsen, A minimum thermodynamic model for the bipolar seesaw. *Paleoceanography* **18**, 1087 (2003).

50. S. A. Marcott, P. U. Clark, L. Padman, G. P. Klinkhammer, S. R. Springer, Z. Liu, B. L. Otto-Bliesner, A. E. Carlson, A. Ungerer, J. Padman, F. He, J. Cheng, A. Schmittner, Ice-shelf collapse from subsurface warming as a trigger for Heinrich events. *Proc. Natl. Acad. Sci. U.S.A.* **108**, 13415–13419 (2011).

51. S. Weldeab, T. Friedrich, A. Timmermann, R. R. Schneider, Strong middepth warming and weak radiocarbon imprints in the equatorial Atlantic during Heinrich 1 and Younger Dryas. *Paleoceanography* **31**, 1070–1082 (2016).

52. S. Barker, P. Diz, Timing of the descent into the last Ice Age determined by the bipolar seesaw. *Paleoceanography* **29**, 489–507 (2014).

53. J. Mignot, A. Ganopolski, A. Levermann, Atlantic subsurface temperatures: Response to a shutdown of the overturning circulation and its recovery. *J. Climate* **20**, 4884–4898 (2007).

54. C. He, Z. Liu, J. Zhu, J. Zhang, S. Gu, B. L. Otto-Bliesner, B. Esther, C. Zhu, Y. Jin, J. Sun, North Atlantic subsurface temperature response controlled by effective freshwater input in “Heinrich” events. *Earth Planet. Sci. Lett.* **539**, 116247 (2020).

55. C. Zhu, J. Zhang, Z. Liu, B. L. Otto-Bliesner, C. He, E. Brady, R. Tomas, Q. Wen, Q. Li, C. Zhu, S. Zhang, L. Wu, Antarctic warming during Heinrich Stadial 1 in a transient isotope-enabled deglacial simulation. *J. Climate* **35**, 3753–3765 (2022).

56. H. Yang, G. Lohmann, C. Stepanek, Q. Wang, R. X. Huang, X. Shi, J. Liu, D. Chen, X. Wang, Y. Zhong, Q. Yang, Y. Bao, J. Müller, Satellite-observed strong subtropical ocean warming as an early signature of global warming. *Commun. Earth Environ.* **4**, 178 (2023).

57. T. Andrews, J. M. Gregory, D. Paynter, L. G. Silvers, C. Zhou, T. Mauritsen, M. J. Webb, K. C. Armour, P. M. Forster, H. Titchner, Accounting for changing temperature patterns increases historical estimates of climate sensitivity. *Geophys. Res. Lett.* **45**, 8490–8499 (2018).

58. M. Winton, K. Takahashi, I. M. Held, Importance of ocean heat uptake efficacy to transient climate change. *J. Climate* **23**, 2333–2344 (2010).

59. D. Baggenstos, M. Häberli, J. Schmitt, S. A. Shackleton, B. Birner, J. P. Severinghaus, T. Kellerhals, H. Fischer, Earth's radiative imbalance from the Last Glacial Maximum to the present. *Proc. Natl. Acad. Sci. U.S.A.* **116**, 14881–14886 (2019).

60. T. L. Rasmussen, E. Thomsen, T. C. E. van Weering, L. Labeyrie, Rapid changes in surface and deep water conditions at the Faeroe Margin during the last 58,000 years. *Paleoceanography* **11**, 757–772 (1996).

61. D. W. Oppo, W. B. Curry, J. F. McManus, What do benthic $\delta^{13}C$ and $\delta^{18}O$ data tell us about Atlantic circulation during Heinrich Stadial 1? *Paleoceanography* **30**, 353–368 (2015).

62. T. Dokken, E. Jansen, Rapid changes in the mechanism of ocean convection during the last glacial period. *Nature* **401**, 458–461 (1999).

63. D. W. Oppo, W. Lu, K.-F. Huang, N. E. Umling, W. Guo, J. Yu, W. B. Curry, T. M. Marchitto, S. Wang, Deglacial temperature and carbonate saturation state variability in the tropical Atlantic at Antarctic Intermediate Water depths. *Paleoceanography* **38**, e2023PA004674 (2023).

64. C. Rühlemann, S. Mulitza, G. Lohmann, A. Paul, M. Prange, G. Wefer, Intermediate depth warming in the tropical Atlantic related to weakened thermohaline circulation: Combining paleoclimate data and modeling results for the last deglaciation. *Paleoceanography* **19**, PA1025 (2004).

65. D. P. Schrag, J. F. Adkins, K. McIntyre, J. L. Alexander, D. A. Hodell, C. D. Charles, J. F. McManus, The oxygen isotopic composition of seawater during the Last Glacial Maximum. *Quat. Sci. Rev.* **21**, 331 (2002).

66. K. Lambeck, H. Rouby, A. Purcell, Y. Sun, M. Sambridge, Sea level and global ice volumes from the Last Glacial Maximum to the Holocene. *Proc. Natl. Acad. Sci. U.S.A.* **111**, 15296–15303 (2014).

67. T. M. Marchitto, W. B. Curry, J. Lynch-Stieglitz, S. P. Bryan, K. M. Cobb, D. C. Lund, Improved oxygen isotope temperature calibrations for cosmopolitan benthic foraminifera. *Geochim. Cosmochim. Acta* **130**, 1–11 (2014).

68. N. J. Shackleton, Attainment of isotopic equilibrium between ocean water and the benthonic foraminifera genus Uvigerina: Isotopic changes in the ocean during the last glacial. *Colloques Internationaux du C.N.R.S* **219**, 203–209 (1974).

69. W. R. Peltier, D. F. Argus, R. Drummond, Space geodesy constrains ice age terminal deglaciation: The global ICE-6G_C (VM5a) model. *J. Geophys. Res. Solid Earth* **120**, 450–487 (2015).

70. D. Lüthi, M. L. Floch, B. Bereiter, T. Blunier, J. Barnola, U. Siegenthaler, D. Raynaud, J. Jouzel, H. Fischer, K. Kawamura, T. F. Stocker, High-resolution carbon dioxide concentration record 650,000–800,000 years before present. *Nature* **453**, 379–382 (2008).

71. S. Gu, Z. Liu, D. W. Oppo, J. Lynch-Stieglitz, A. Jahn, J. Zhang, L. Wu, Assessing the potential capability of reconstructing glacial Atlantic water masses and AMOC using multiple proxies in CESM. *Earth Planet. Sci. Lett.* **541**, 116294 (2020).

72. F. He, "Simulating transient climate evolution of the last deglaciation with CC SM3," thesis, University of Wisconsin-Madison (2011), pp. 171.

73. J. F. Adkins, K. McIntyre, D. P. Schrag, The salinity, temperature and $\delta^{18}O$ of the glacial deep ocean. *Science* **298**, 1769–1773 (2002).

74. Z. Liu, S. Shin, R. Webb, E. Lewis, B. L. Otto-Bliesner, Atmospheric CO_2 forcing on glacial thermohaline and climate. *Geophys. Res. Lett.* **32**, L02706 (2005).

75. B. L. Otto-Bliesner, C. D. Hewitt, T. M. Marchitto, E. Brady, A. Abe-Ouchi, M. Crucifix, S. Murakami, S. L. Weber, Last Glacial Maximum ocean thermohaline circulation: PMIP2 model intercomparisons and data constraints. *Geophys. Res. Lett.* **34**, L12706 (2007).

76. C. Zhu, Z. Liu, S. Zhang, L. Wu, Global oceanic overturning circulation forced by the competition between greenhouse gases and continental ice sheets during the last deglaciation. *J. Climate* **34**, 7555–7570 (2021).

77. S. G. Valley, J. Lynch-Stieglitz, T. M. Marchitto, Intermediate water circulation changes in the Florida Straits from a 35 ka record of Mg/Li-derived temperature and Cd/Ca-derived seawater cadmium. *Earth Planet. Sci. Lett.* **523**, 115692 (2019).

78. N. E. Umling, D. W. Oppo, P. Chen, J. Yu, Z. Liu, M. Yan, G. Gebbie, D. C. Lund, K. R. Pietro, Z. D. Jin, K.-F. Huang, K. B. Costa, F. A. L. Toledo, Atlantic circulation and ice sheet influences on upper South Atlantic temperatures during the Last Deglaciation. *Paleoceanogr. Paleoclimatol.* **34**, 990–1005 (2019).